Interferometric Tomography Measurement of the Temperature Field in the Vicinity of a Dendritic Crystal Growing from a Supercooled Melt.

I. Braslavsky and S. G. Lipson
Technion - Israel Institute of Technology

Transactions of Optical methods and data processing in heat and fluid flow, IMECHE, London 1998, p. 423-432.

The shape of a crystal growing from a supercooled pure melt is influenced by the temperature-dependent kinetics of the nucleation on the interface. In the course of this growth, heat is released from the interface, thus feeding back on the temperature field. In this intrinsically nonlinear process, the three-dimensional temperature field in the fluid is a vital dynamic parameter which has not been previously measured. This can be done with the aid of multi-directional interferometry, using the temperature dependence of the refractive index of the melt. If the growth regime lies in the path of one of the interferometer beams, a phase shift, proportional to the integrated refractive index change, is observed. To measure the three-dimensional field of the refractive index requires some form of tomographic reconstruction. We built an apparatus that includes a crystal growing cell which is viewed by four Mach-Zehnder interferometers. The interferograms are analyzed by Fourier fringe analysis, and the field is reconstructed by the algebraic reconstruction technique (ART), an algorithm which has been shown by Verhoeven to be suitable for limited data tomography. Measured temperature fields around growing crystals of *heavy ice* (D_2O) and *succinonitrile* are presented. Internal self-consistency of the field magnitudes is demonstrated, without the need for adjustable parameters.

1. INTRODUCTION

The growth of crystals from a supercooled melt is a broad subject which has been researched for several decades[1-7]. A crystal is nucleated in a supercooled melt at uniform temperature and begins to grow. Latent heat is ejected from its surface and is transported away by conduction through the fluid. The rate at which the crystal grows is controlled by the surface

heat flux and the temperature dependence of the interface growth processes. The problem has aroused considerable mathematical interest because it involves deterministic field equations which have to be solved together, and which create their own boundary conditions (the Stefan problem). The solution of the problem also has considerable practical importance in metallurgy. It is known that, under specified boundary conditions, a single growth mode (velocity, shape) is selected, although proof of this has turned out to be a most difficult mathematical nut to crack.

The shapes of crystals growing under such conditions are almost always dendritic (tree-like). The shapes and velocities of dendritic crystals have been measured for different materials such as succinonitrile[8,9], pivalic acid[10] (both plastic solids), xenon[11] ice[12,13], and heavy ice[14]. Measurements of the temperature field in the melt have not been made previously. These fields are important since they indicate the boundary conditions which are an integral part of the problem, and are usually not known. In the case of salt crystals growing from supersaturated solution, which pose a similar problem, concentration fields around growing crystals have been measured in a few cases[15]. This has been done by interference microscopy in quasi-two-dimensional systems (a thin growth cell in the focal plane of the microscope), using the linear relationship between refractive index and solution concentration. However, two-dimensional growth from the melt is not possible because the boundaries of a thin cell create conditions which are quite different from those of the free growth problem. Measurements of the fields in growth from the melt must therefore be done in a three-dimensional environment.

Many experiments have measured three-dimensional temperature fields using the relationship between refractive index and temperature.[16-20] Since interferometry can be used to measure the integrated value of refractive index along a given optical path, it is usually necessary to extract the field by tomographic inversion. Still, under some circumstances, useful information can be obtained directly from the projections. Several investigations have used double-exposure holographic interferometry to record the optical paths in several directions simultaneously in a single picture. However, the double-exposure method compares waves at only two distinct times, and cannot be used to investigate the complete time-development of the field. Real-time holographic interferometry, which in principle records the time-development, does not allow post-factum determination of optical paths in several directions as does the double-exposure method, and therefore has no advantages over the interferometric technique to be described below.

When a crystal grows, the length-scale of the temperature field in the fluid around it is determined by the *diffusion length* $l_D = 2D/v$ where D is the diffusion constant (heat or mass) and v is the velocity of growth. In the experiments to be described here on ice, diffusion lengths are of the order of 0.5mm. This figure, together with the depth of field required to observe a rapidly-growing crystal from several directions simultaneously determines the optical magnification which can be used. The experimental method to be discussed here involves imaging the crystal through Mach-Zehnder interferometers from four directions simultaneously, and using a tomographic reconstruction program devised by Verhoeven [21] and shown by him to be optimized for this rather small number of directions. The field of view obtained was about 10mm diameter.

2. EXPERIMENTAL SET UP

The experimental set-up allows the crystal to be nucleated and grown in a temperature controlled environment and to be monitored by four vertical Mach-Zehnder interferometers. The growth vessel is a glass cylinder inside a perspex container through which a cooling

mixture is circulated. Eight access windows are constructed from perspex tubes with flat window ends and filled with air which is dried in order to avoid condensation. Because of the need to construct four interferometers within a small space, each one is laid out in a vertical plane (Figure 1), so that the four reference beams, which bypass the experimental chamber, lie in a plane above the cell. After recombination of the beams in each interferometer, a lens system focuses the image of the center of the cell onto one quadrant of a 512 X 512 CCD. Each lens system includes a cylindrical lens to correct for distortion by the cylindrical cell. The complete optical layout is shown in Figure 2. The four interferometric images thus obtained are electronically combined into a single video frame and recorded simultaneously on a VCR. The temperature of the circulation bath can be maintained to an accuracy of 0.01°C. Crystals are nucleated in a capillary tube terminating at the center of the field of view. In the case of ice crystals, an electro-freezing device[22] is used for nucleation at supercooling greater than 0.1°C. In the case of succinonitrile local cooling by a Peltier cooler is used to initiate the growth.

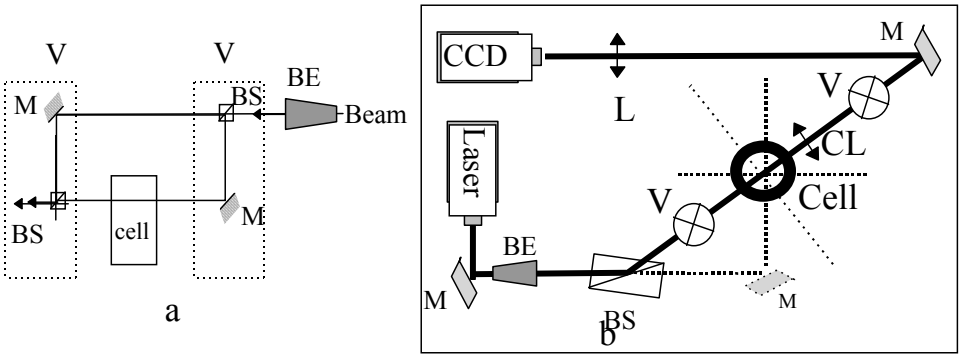

Figure 1. Vertical Mach-Zehnder interferometer: (a) side view of one interferometer (b) top view of the optical set up for one interferometer. [Components include: mirrors (M), beam splitters (BS), beam expander (BE), cylindrical lens (CL), imaging lens (L), Argon laser, and a CCD camera. Where V indicates BS & M, one above the other.]

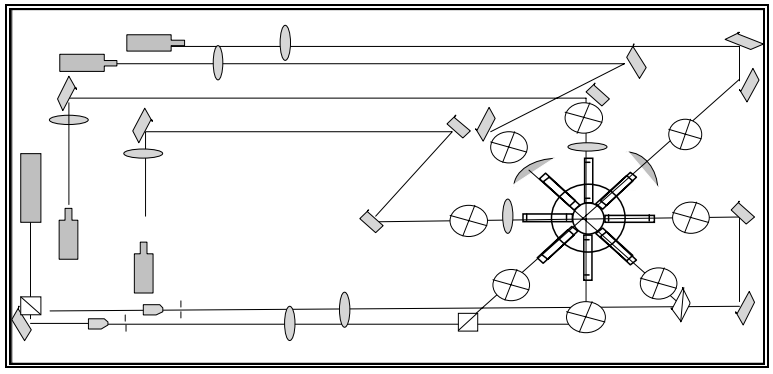

Figure 2. The full optical setup includes four interferometers, the growth cell is situated in the optical path of all four.

3. INTERFEROMETRIC TOMOGRAPHY

3.1. Interferometric analysis

The method by which a single interferogram is analysed has been described by Kostianovski et al.[23] When an interferometer is aligned correctly and there is no crystal in the field of

view (i.e., the fluid has uniform temperature), one would expect a uniformly-spaced set of interference fringes to be obtained. However, this is often not the case, because of optical imperfections. For this reason, an "empty-field" interferogram is taken from the recording immediately before the emergence of the crystal. During the growth process, the interference fringes become distorted, and the difference in phase $\Delta\phi$ (*x, y*) at point (*x, y*) in the field of view is determined by the Fourier transform method[23]. This phase difference is related to the refractive index field *n* (*x, y, z*) by an integral along the line of sight, which is assumed to be a straight line because the index gradients are small. The phase difference is given by:

$$\Delta\phi(x,y,t) = \frac{2\pi}{\lambda}\int (n(x,y,z,t) - n_\infty)dz \quad (1)$$

$$\Delta\phi(x,y,t) = \frac{2\pi}{\lambda}\int (\frac{\partial n}{\partial T}(T(x,y,z,t) - T_\infty)dz \quad (2)$$

In the latter equation, a linear relationship between the temperature *T* and the refractive index has been assumed. This is not always the case, for example in water around the maximum in refractive index[24] at 0.1°C; but it is easy enough to use a more exact relationship.

The Fourier transform method of determining $\Delta\phi$ is a mathematical equivalent to image-plane holographic interferometry. The empty-field interferogram is denoted by g_0 (*x, y*) and that with the crystal is in the field of view by *g* (*x, y*). These are given schematically by

$$g_0(x,y) = a(x,y) + b(x,y)\cos[2\pi f_0 x + \phi_0(\mathrm{x,y})] \quad (3)$$

$$g(x,y) = a(x,y) + b(x,y)\cos[2\pi f_0 x + \phi(\mathrm{x,y})] \quad (4)$$

in which we substitute

$$\phi(\mathrm{x,y,t}) = \phi_0(\mathrm{x,y}) + \Delta\phi(\mathrm{x,y,t}) \quad (5)$$

The two-dimensional Fourier transforms of (3) and (4) are calculated, and by retransforming the first order peaks only, the phases ϕ_0 (*x, y*), ϕ (*x, y*) and thus $\Delta\phi$ are calculated. The first stage of the process is shown schematically in Figure 3, in which examples of interferograms before and during the crystal growth are shown, together with their Fourier transforms. By this method a resolution in phase of the order of 0.06 rad can be obtained[23].

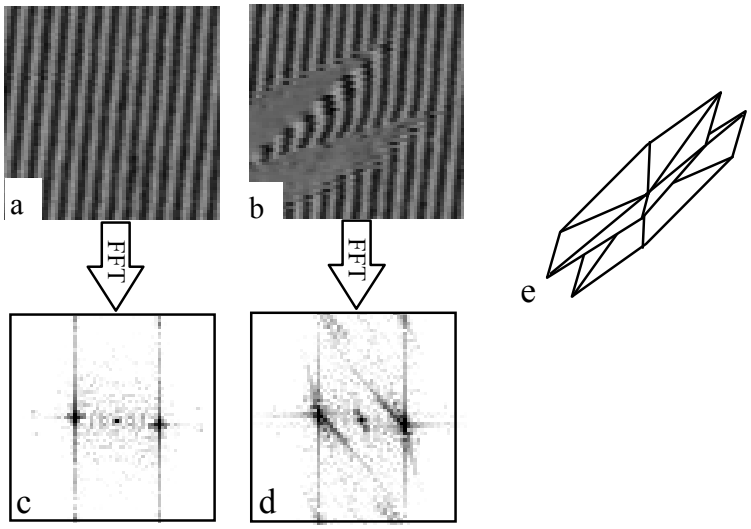

Figure 3. Interferograms recorded and transformed during growth of a heavy-ice crystal. (a) The empty-field interferogram; (b) Interferogram including projection of a double-pyramidal crystal; (c) Modulus of the two-dimensional Fourier transform of (a); (d) Modulus of the two-dimensional Fourier transform of (b). (e) The double-pyramid structure of ice crystals.

3.2. Tomographic reconstruction

The method of tomography creates the three-dimensional map of the refractive index from several two-dimensional projections. Many different procedures for doing this have been published [25, 26]. In general, the larger the number of projection directions, the better the accuracy of the resulting field. The present problem is limited by the small number of viewing directions available, and by the fact that parts of the field become obscured as the crystal grows. Verhoeven[21] has compared several possible algorithms which can be applied to such a problem and found that the "algebraic reconstruction technique" (ART) [27] and "multiplicative algebraic reconstuction technique" (MART) can successfully used under these conditions. We have confirmed, by simulation experiments, that these techniques can be applied successfully with as few as four access directions, although the accuracy is compromised. Mewes et al.[28] have also applied the same algorithms to tomographic reconstuction from limited data sets obtained from double-exposure holography. They also conclude that four directions are sufficient in order to determine the temperature field.

The general principle of these algorithms is to begin with an arbitrary trial field. One then calculates the projection of this field in the direction of the first projection. The field values are corrected uniformly along the projection axis in order to match the data in this direction. The projection from this field is now calculated along a second direction, and the field adjusted again to match the data; this of course spoils the match along the first direction. The process is repeated for all the projection directions and then iterated many times, until the mean square change between iterations reaches a minimum. Because of the small number of projections, the inversion problem is under-determined. This algorithm has been shown to find the solution with minimum variance, which is a physically reasonable solution for problems in which one expects smooth variations in the field.

4. TEMPERATURE AROUND A POINT SOURCE

In order to confirm the ability of the system to reconstruct a temperature field from four measured projections, an experiment was performed using a small heater in water. A complete check of the result would include comparison with the same field measured by point thermistors, but in this case the scale of the field resolution required (0.1 mm) precluded such a test because of the size of the thermistors and the influence of the necessary wiring. The field determined experimentally was therefore compared to that calculated analytically for the same system. The temperature field is measured around a point heater emitting power Q, at time t_o after it was switched on. The Green function for this field is given by:

$$G(\vec{r},t_o)=\frac{Q}{C}\frac{1}{(4\pi Dt)}\exp[-\frac{\vec{r}^{\,2}}{4Dt}] \qquad (6)$$

and integration from $t = 0$ to $t = t_o$ gives the field:

$$T(\vec{r},t_o)-T_\infty=\frac{Q}{C4\pi D}\cdot\frac{1}{|\vec{r}|}\cdot\left(1-\mathrm{erf}\left(\frac{|\vec{r}|}{\sqrt{4Dt_0}}\right)\right) \qquad (7)$$

where C is the specific heat. (This field can be appreciated intuitively as the Laplacian field $(1/|r|)$ with a cut-off at the diffusion length $(4D\,t_0)^{1/2}$ where $D = \kappa/C\rho$.) Figure 4 shows the four projections of the field around the point heater as contour maps of $\Delta\phi$, and one section. One should notice that parts of the fields are obscured by the resistor and its wires.

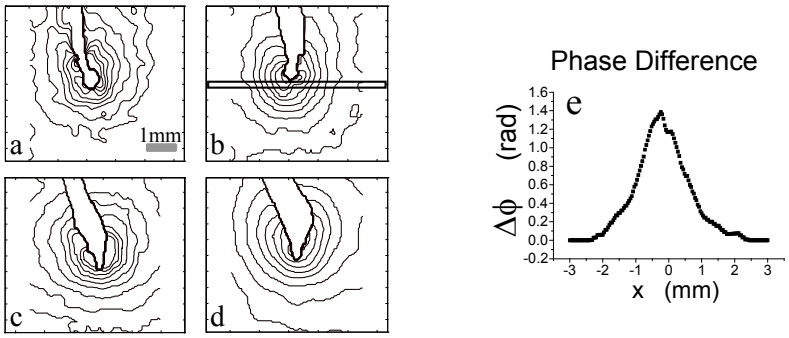

Figure 4. (a-d) The refractive index projections from four directions in the vicinity of a 0.3mm heater immersed in water. (e) The profile below the heater along the line in (b).

Figure 5(a) shows the horizontal cross-section of the reconstructed temperature field, in the plane of the four observation directions, just below the resistor. This figure indicates the degree to which the small number of observation directions affects the apparent uniformity of the field. Figure 5(b) shows the profile of this field along the double line in 5(a), as compared with eq. (7), with no adjustable parameters. It should be pointed out that the center of the heat distribution appears experimentally to be 0.5 mm above the base of the resistor, presumably because of Archimedean buoyancy of the heated water.

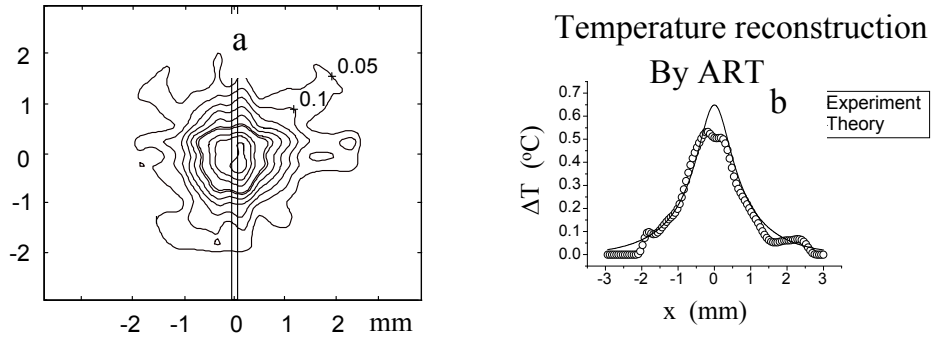

Figure 5. The reconstructed field, (a) A horizontal slice from the field. (b) A comparison with the prediction along a section in (a).

5. DENERITIC GROWTH

The problem of morphology and fields around dendritically growing crystals has been reviewed by Ben-Jacob [5]. During dendritic growth the crystal shape and the fields around it are expected to move along the growth axis with translational invariance. Although this has been confirmed for the external profile of several crystals, there is as yet little information on the fields. We have carried out experiments on two materials which are quite different in their growth behaviour: ice, which is very anisotropic, and succinonitrile, which has a small anisotropy and has become a standard material for quantitative studies of dendritic growth. These experiments are only preliminary, but suggest that the techniques developed here can be used advantageously for further work.

5.1. Succinonitrile

Succinonitrile was used for experiments not only because it has become a standard material, in dendritic growth investigation [8], but also because the dependence of its refractive index on temperature around the melting point is large[29] compared to other materials. Figure 6 shows an example interferogram and the phase differences $\Delta\phi$ deduced from it (and from the corresponding empty field). The signal-to-noise ratio of this interferogram is very high, and values of $\Delta\phi$ in excess of 6π are indicated. In order to avoid problems of obscuration, the data was analyzed in the lower region of the interferograms, below the lowest tip, where all values of $\Delta\phi$ are less than 2π, which also simplifies the analysis. The corresponding tomographic reconstructions are shown in Figure 7(b). Three dimensional field maps for materials with anisotropy similar to that of succinonitrile have been calculated analytically by Ben-Amar [30] and numerically by Kobayashi [31]; these will be compared quantitatively in the near future.

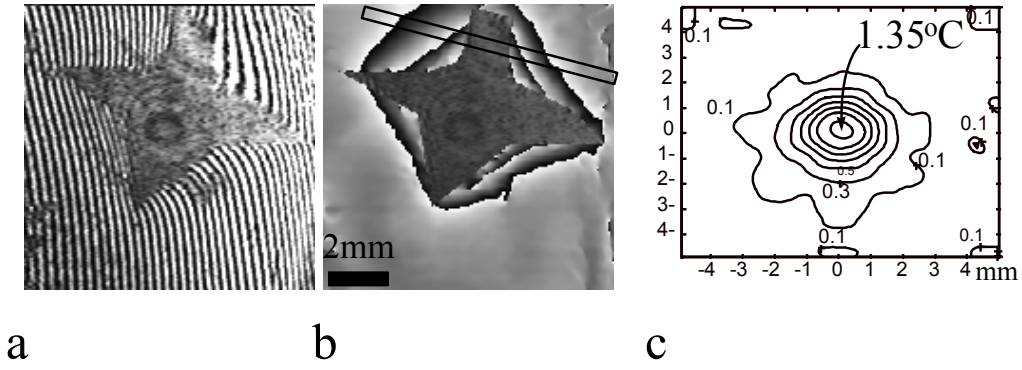

Figure 6. (a) Interferogram of a succinonitrile crystal growing at 1.4°C supercooling. (b) The calculated $\Delta\phi$ modulo 2π, shown as gray-scale. (c) Field calculated using symmetry considerations and interpolation of $\Delta\phi$ in the obscured region.

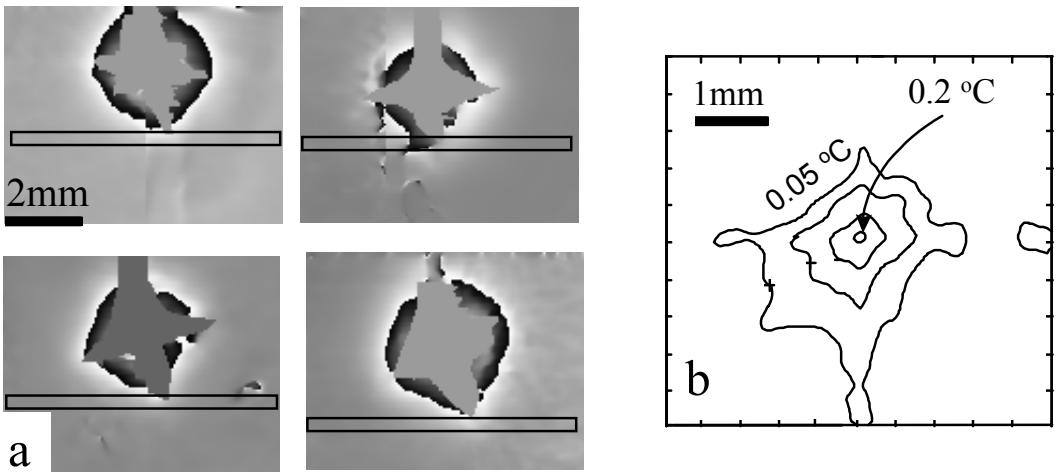

Figure 7. (a) Phases $\Delta\phi$ for four projections around a succinonitrile crystal growing at 1.3°C supercooling . (b) Temperature field calculated from (a) in the plane below the dendrite tip.

5.2. Heavy water

The growth of ice crystals, the first dendritic crystals ever to be studied, shows several interesting features, which were the original impetus for this work. Unfortunately, it appears that the refractive index of water[24] has its maximum value at 0.1°C, which means that the sensitivity to temperature fields is very poor at small supercoolings. For this reason, experiments were carried out on the growth of *heavy* ice crystals, since *heavy* water has a maximum refractive index[32] at 6.75°C whereas its melting point is 3.81°C. Even so, the value of *dn/dT* is an order of magnitude less than that of succinonitrile at its melting point. Moreover, the full relationship *n(T)* has to be taken into account.

A feature of ice crystals which is of particular interest is the phenomenon of pyramidal growth[33]. Ice crystals grow as dendritic structures with hexagonal symmetry, and because the anisotropy is very great and growth along the hexagonal axis is much slower than in

directions normal to it, the outer shape of the dendritic structure is a hexagonal plate. However, when the supercooling is greater than 2.75°C the hexagonal plate splits into two hexagonal pyramids, joined at their apices, which are mirror images of one another (see Figure 3(e)). The reason for this form of growth is not clear. Suggestions [33, 34] have been put forward which imply that an asymmetry in the temperature field is involved in it. We have therefore concentrated on measuring the temperature field around the pyramids in the temperature region where the phenomenon appears. The spatial resolution obtained was insufficient to show details of the field at the growth edge, where l_D is of order 0.05 mm, but the fields can be measured on a coarser scale. The region between the pyramids was almost impossible to view from more than one direction without obscuration. However, it is possible to obtain meaningful data from one projection on the assumption that if the crystal were oriented with the hexagonal axis exactly vertical, three observation directions at 120° would see the same profile. By using the known symmetry of the crystal together with the one unobscured projection, it was therefore possible to deduce the temperature field using the tomographic algorithm. This method was also used to obtain the field shown in Figure 6(c).

The results, shown in Figure 8, were obtained from the interferograms shown in Figure 3. The results show that the water is at the melting temperature between the pyramids, close to the apices. This, by itself, is an independent check of the calibration of the system, since equilibrium is established in regions where the crystal is no longer growing. Figure 8(a) indicates the degree of asymmetry of the field around the growing crystal tip. In Figure 8(c), one should remark that the hexagonal symmetry observed is the consequence of the method used.

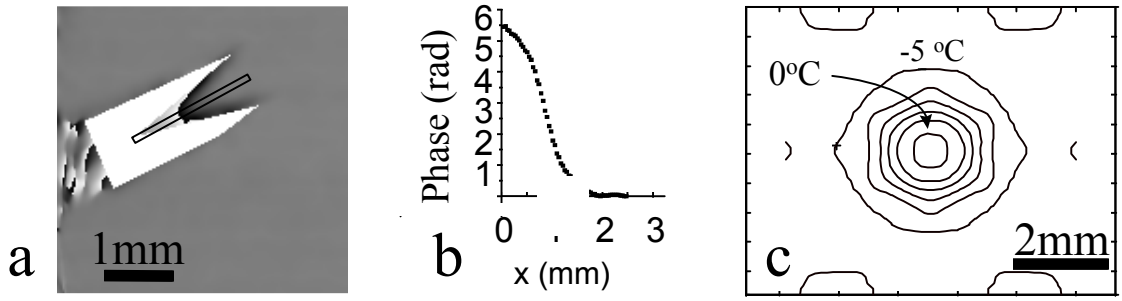

Figure 8. (a) The Phase $\Delta\phi$. (b) Profile from a slice in the middle of the double pyramid structure of ice growing in supercooled heavy water at 5.3°C below the melting point. (c) Reconstructed field in a plane at the middle of the double-pyramid structure.

6. CONCLUSION

In this paper we have presented an experimental method and preliminary results of measuring the three-dimensional temperature fields around crystals growing from supercooled melts. The three-dimensional nature of the fields makes their measurement considerably more difficult than that of the two-dimensional fields around crystals growing from solution. Despite this difficulty, the results appear to be significant, and the technique has potential for further development.

Acknowledgments: We acknowledge helpful discussions with Dean Verhoeven, who also supplied us with algorithms for the tomographic reconstruction. In addition we want to thank

Michael Elbaum and Jonathan Bar-Sagi for suggestions to Shmuel Hoida and Yoram Garnizky for technical support and to Henry Fenichel and Netta Cohen for reading critically the manuscript. This research was partially supported by the German-Israel Binational Science Foundation (GIF), the Fund for Basic Research of the Israel Academy of Sciences and the Minerva Center for Non-linear Research.

REFERENCES

[1]G. P. Ivantsov, Dokl. Akad Nauk. SSSR **58**: 567 (1947).
[2]W.W Mullins and R.F Sekerka. J Appl. Phys., **34**:323, (1963) ; **35**:444, (1964).
[3]J.S. Langer and H. Müller-Krumbhaar, Acta Metall. **26**:1681 (1978).
[4]D. A. Kessler, J. Koplik, and H. Levin, Phys Rev A **33**:3352 (1986).
[5]E. Ben-Jacob, Contemp. phys., **34**:247 (1993).
[6] R. Kupferman, D.A. Kessler, and E. Ben-Jacob Physica A **213**: 451 (1995).
[7]E. Brener, H. Müller-Krumbhaar, and D. Temkin, Physical Review E, **54**:2714 (1996).
[8]M.E. Glicksman, R.J. Schaefer, and J.D. Ayers.. Metall. Trans. **A 7**:1747 (1976).
[9]M.E. Glicksman, M. B. Koss, E. A. Winsa, Phys. Rev. Lett **73**:573 (1994).
[10]A. Dougherty, J. Cryst. Growth **110**:501 (1991).
[11]U. Bisang and J. H. Bilgram, Phys. Rev. E. **54**:5309 (1996).
[12]K. K. Koo, R. Ananth, and W. Gill, Phys. Rev. A **44**:3782 (1991).
[13]W. Shimada and Y. Furukawa, J. Phys Chem. B **101**:6171 (1997).
[14]I. Braslavsky and S. G. Lipson, Physica A **249**:190 (1998).
[15]E. Raz, S. G. Lipson, and E. Polturak, Phys. Rev. A **40**:1089 (1989).
[16]D. Mewes and R. Renz , Chem.Ing.Tech.**63**:699 ,(1991).
[17]S. Bahl and J. A. Liburdy, Int. J. Heat Mass Transfer **34**:949 (1991).
[18]Y. Zhang and G. A. Ruff, Meas. Sci Technol. **5**:495 (1994).
[19]Y. C. Michael, K. T. Yang, Transactions of the ASME, J. of Heat Transfer. **114**:622 (1992).
[20]D. Shi, S. Chen, R. Wang, X. Xiao, Appl. Optics. **34**:3064 (1995).
[21]D. Verhoeven, Appl. Opt. **32**:3736 (1993).
[22]I. Braslavsky and S. G. Lipson, Appl. Phys. Lett. **72**:264 (1998).
[23]S. Kostianovski, S. G. Lipson, and E. N. Ribak, Appl. Optics **32**:4744 (1993).
[24]Ch. Saubade, J. Physique **42**:359 (1981).
[25]A. C. Kak and M. Slaney ,Principles of Computerized Tomographic Imaging, IEEE Press 1988.
[26]D.W .Sweeney and C.M Vest , App. Opt. **12**:2649 (1973).
[27]Gordon, R., Bender, R. and Herman, G.T , J. Theor. Biol **29**:471 (1970).
[28]D. Mewes and W. Ostendorf , Int. Chem. Eng. **26**:11 (1986).
[29]R. M. Macfarlane, E. Courtens, and T. Bischofberger, Mol. Cryst. Liq. Cryst., **35**:27 (1976).
[30]M. Ben Amar and E. Brener, Phys. Rev. Lett. **71**:589 (1993).
[31]R. Kobayashi, Exp. Math. **3**:59 (1994).
[32]H. Eisenberg, J. Chem. Phys. **43**:3887 (1965).
[33]W. C. Macklin and B. F. Ryan, Phil. Mag. **14**, 847 (1966).
[34]I. Braslavsky and S. G. Lipson, To be published.